Available online at www.sciencedirect.com
ScienceDirect
Journal of Hazardous Materials 154 (2008) 21–28
Journal of Hazardous Materials
www.elsevier.com/locate/jhazmat

Adsorption of selected volatile organic vapors on multiwall carbon nanotubes

Yang-hsin Shih [a,*], Mei-syue Li [b]

[a] *Department of Soil and Environmental Sciences, Center of Nanoscience and Nanotechnolgy, National Chung Hsing University, Taichung 402, Taiwan, ROC*
[b] *Department of Soil and Environmental Sciences, National Chung Hsing University, Taichung 402, Taiwan, ROC*

Received 23 March 2007; received in revised form 24 August 2007; accepted 24 September 2007
Available online 29 September 2007

Abstract

Carbon nanotubes are expected to play an important role in sensing, pollution treatment and separation techniques. This study examines the adsorption behaviors of volatile organic compounds (VOCs), *n*-hexane, benzene, trichloroethylene and acetone on two multiwall carbon nanotubes (MWCNTs), CNT1 and CNT2. Among these VOCs, acetone exhibits the highest adsorption capacity. The highest adsorption enthalpies and desorption energies of acetone were also observed. The strong chemical interactions between acetone and both MWCNTs may be the result from chemisorption on the topological defects. The adsorption heats of trichloroethylene, benzene, and *n*-hexane are indicative of physisorption on the surfaces of both MWCNTs. CNT2 presents a higher adsorption capacity than CNT1 due to the existence of an exterior amorphous carbon layer on CNT2. The amorphous carbon enhances the adsorption capacity of organic chemicals on carbon nanotubes. The morphological and structure order of carbon nanotubes are the primary affects on the adsorption process of organic chemicals.

Keywords: Carbon multiwall nanotubes; Adsorption; Volatile organic compounds

1. Introduction

Volatile organic compounds (VOCs) are used in both domestic and industrial applications, including transport, household chemicals, paints and adhesives. VOCs are also an important class of chemical pollutants in the environment due to their high volatility. Since the existence of VOCs in the atmosphere causes severe health problems, they have attracted public and academic attention. Many VOCs and their degradation products are known or suspected carcinogens, and the development of effective treatments to remove these organic chemicals is necessary.

One method of controlling VOC emissions is adsorption onto carbon sorbent. These sorbents have high removal efficiencies and low cost, which make them cost effective processes that are also able to be regenerated and to recover many VOCs for reuse. However, there are still gaps in our understanding of gas-to-particle partitioning in most carbon adsorbent materials, such as activated carbon, because they are essentially structureless and have complex physicochemical properties. In contrast, carbon nanotubes have well-defined structures. Sorption of VOCs on carbon nanotubes can provide a better understanding of the relationships between sorption potential and carbon structures. Therefore, the adsorption of organic vapors in carbon nanotubes is an important issue for both theoretical study and environmental applications.

Carbon nanotubes (CNTs), originally discovered by Iijima [1], can offer crystalline pores of cylindrical shape with walls consisting mainly of graphite sheets. There are two categories of carbon nanotubes: single-walled carbon nanotubes (SWCNTs) consisting of only one carbon layer and with pores in the microporous range and multiwalled carbon nanotubes (MWCNTs), which consist of at least two layers and have pores in mesopore range. Since the layer-to-layer spacing of 0.34 nm in MWCNTs [2] is generally smaller than the radius of gyration of organic vapors, most organic chemicals are too large to be adsorbed between the MWCNTs layers. Adsorption can occur on the external wall surface of MWCNTs or through capillary condensation in the MWCNTs pores.

* Corresponding author. Tel.: +886 4 22854152; fax: +886 4 22854152.
E-mail address: yhs@nchu.edu.tw (Y.-h. Shih).

0304-3894/$ – see front matter © 2007 Elsevier B.V. All rights reserved.
doi:10.1016/j.jhazmat.2007.09.095

Table 1
Physiochemical properties of selected VOCs

	Molecular formula	Molecular weight (g/mol)	E^a	S^a	A^a	B^a	L^a
TCE	C_2HCl_3	131	0.52	0.37	0.080	0.030	3.0
Benzene	C_6H_6	78.1	0.61	0.52	0.00	0.14	2.8
n-Hexane	C_6H_{14}	86.2	0.00	0.00	0.00	0.00	2.7
Acetone	C_3H_6O	58.1	0.040	0.70	0.49	0.55	1.8

[a] Parameters of linear solvation energy relationships (LSER) [53]. *E* reflects the ability of the solute to interact with a sorbent through π- and n-electron pairs. *S* is the solute dipolarity/polarisability parameter. *A* is a measure of the solute hydrogen-bond acidity. *B* is a measure of the solute hydrogen-bond basicity. *L* is the solute gas–liquid partition coefficient on *n*-hexadecane at 25 °C.

In recent years CNTs have been proposed as adsorbents for a variety of gases, such as hydrogen [3], NH_3 and NO_2 gas [4] by SWCNTs, as well as ethanol, *n*-hexane [5], *n*-nonane and CCl_4 [6]. Carbon nanotubes have a higher removal efficiency of dioxin than activated carbons [7]. Crespo and Yang [8] showed that the adsorption capacity of single-wall carbon nanotubes for thiophene is larger than that of activated carbons. Peng et al. [9] found that carbon nanotubes efficiently adsorb 1,2-dichlorobenzene in water at pH 3–10. The adsorption volume of PAHs on carbon nano-materials is decreased with molecular volume and adsorption volume on carbon nanotubes is much higher than fullerence [10]. However, there has been limited investigation of the adsorption of VOCs vapors with MWCNTs.

This study aims to investigate the adsorption mechanisms and thermodynamics of four volatile organic vapors, trichloroethylene, *n*-hexane, benzene and acetone on multiwalled nanotubes. Four organic compounds with different chemical moieties were used as chemical probes to study the adsorption interactions on two MWCNTs. The heat of adsorption of these organic chemicals was also analyzed. These parameters are useful in predicting the performance of these adsorbents and facilitating the design of adsorption systems.

2. Materials and methods

2.1. Materials

The four tested VOCs, trichloroethylene (purity > 99.5%), benzene (purity > 99.9%), acetone (purity > 99%), and *n*-hexane (purity > 99%), were of gas chromatographic analytical grade and purchased from Aldrich. These four VOCs have similar molecular size but they belong to different organic groups (Table 1). Trichloroethylene, a chlorinated alkene, and benzene, an aromatic organic compound, are common organic contaminants in the environment. Acetone, a ketone, and *n*-hexane, a linear alkane, are widely used industrial solvents. Two carbon multiwall nanotubes, CNT1 and CNT2, were purchased from Aldrich in different batch with purity higher than 95 wt.%. These two MWCNTs have similar diameters and lengths, and were used without further purification.

2.2. Characterization of MWCNTs

The multiwall carbon nanotubes were characterized to analyze their geometrical structure and surface properties including: surface area, pore volume, and surface carbon properties. The morphologies and microstructures were studied with a scanning electron microscope (SEM, TOPCON, ABT-150S Thermionic Emission SEM, Japan), with an energy dispersive spectrometer (EDS) and with a high-resolution transmission electron microscope (HRTEM, JEM-2010, JEOL Ltd., Japan). The nitrogen adsorption isotherm at 77 K was determined using a Micromeritics ASAP2100 analyzer accelerated surface area and porosimetry apparatus. The sample was degassed at 378 K for 1 h. Confocal Raman spectra and images (Nanofinder-30, Tokyo Instruments Inc., Japan) were measured by HeNe laser excitation at 632.8 nm. The X-ray photoelectron spectroscopy (XPS) was performed with a VG-Scientific ESCALAB 250 spectrometer (UK) with monocromatized Al Kα X-ray source.

2.3. Adsorption experiments

The adsorbent was placed into a 10 cm length of stainless steel column (o.d. 1/8 in.). In order to obtain homogeneous packing, the adsorbent was introduced in small quantities, accompanied by mechanical vibration. The two ends of the column were plugged with silane-treated glass wool. The columns loaded with around 10 mg MWCNTs were then stabilized in a conventional gas chromatograph (Model 8700F, Taiwan) at 453 K overnight under a helium flow rate of 5–60 mL/min. The gas chromatograph was equipped with a flame ionization detector (FID). Nitrogen (purity >99.995%) was used as carrier gas, and flow rates of 5–10 mL/min were measured using a calibrated soap bubble flowmeter. All measurements were performed in an isothermal oven in the temperature range of 303, 333, and 363 K. In order to meet the requirements for adsorption at infinite dilution, symmetry of the peaks and retention time reproducibility, the injection amounts were in the range from 1 to 100 μL gases. This was also examined by varying the carrier gas velocity and the vapor concentration. Injection amounts in the range from 0.5 to 1000 μL of organic vapor have been suggested to allow measurements at infinite dilution conditions and in the Henry's law region for the determination of adsorption coefficients on mineral surfaces [11] and black carbons [12]. Methane was used as a marker for retention time correction.

The equilibrium sorption isotherm can be assumed to be linear and can be described by a sorption coefficient because of the low concentrations of contaminants usually present in the environment. Adsorption coefficients (K_s) can be described by the equation, $K_s = C_s/C_g$, where C_s is the concentration of solute in the solid phase and C_g is the concentration of solute in the gas phase. The inverse gas chromatography (IGC) method [13,14]

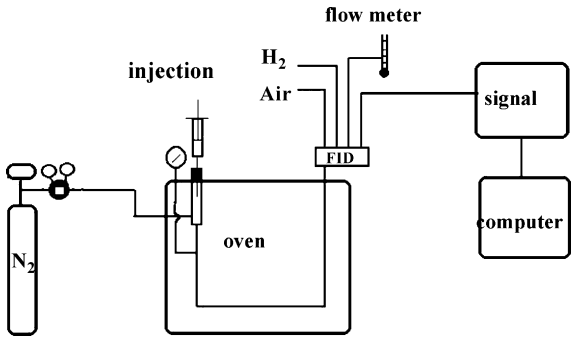

Fig. 1. A schematic experimental setting of inverse gas chromatography.

has been widely used for low concentrations to study gaseous sorption on solids. After the injection of the probe molecule, adsorption takes place on the carbon sorbents in the column followed by desorption. The schematic experimental setting is shown in Fig. 1. IGC has been widely utilized to study various materials, such as carbon blacks [15], activated carbons [16], organoclays [17], and fibers [18].

In this chromatographic method, a chemical molecular probe i is injected into the column under isothermal conditions and the observed retention is a measure of its sorption intensity. The net retention volume (V_N) is determined using the follow relation:

$$V_N = (t_R - t_M)JTF \quad (1)$$

where t_R is retention time of chemical, t_M is retention time of an inert tracer (i.e., methane), J is a correction term for the pressure drop across the column, T is a correction term for the temperature, and F is flow rate.

At an infinitely dilute adsorbate concentration, the adsorption coefficients are related to V_N by the following [11,12,14]:

$$V_N = K_s M \quad (2)$$

where M is the mass of adsorbent in the column.

The volumetric flow rate of the carrier gas is corrected by the pressure drop in a chromatographic system. For each measurement, at least three repeated injections were taken to obtain reproducible results.

Temperature-programmed desorption (TPD) was performed using a gas chromatograph (Agilent 6890, USA) equipped with a FID detector. TPD has been adopted by several researchers to screen adsorbents for organic chemicals and study the interactions of organic chemicals on carbon nanotubes [7,19,20]. In short, small amounts of VOC chemicals were loaded onto the two MWCNTs and columns were then purged with helium at room temperature. As oven temperature is increased, the adsorbed VOC chemical eventually desorbs. The rate of desorption increases initially and reaches a maximum rate at a specific temperature and then decreases. Because this desorption peak temperature is related to the adsorption bond strength, a stronger bond gives rise to a higher TPD temperature [21]. In the absence of readsorption from the gas phase, the rate of desorption is [21]

$$-\frac{d\theta}{dt} = k_d e^{-E/RT}\theta \quad (3)$$

where θ is the fractional surface coverage, T is the temperature, t is the time, E is the activation energy for desorption, R is the gas constant, and k_d is a constant that depends on the desorption kinetics. The activation energy for desorption is calculated by [22]

$$2 \ln T_m - \ln b = \frac{E}{RT_m} + \ln A \quad (4)$$

where T_m is the peak desorption temperature, b is the heating rate and A is a constant.

3. Results and discussion

3.1. MWCNT morphology

Two multiwall carbon nanotubes, CNT1 and CNT2, were examined by a high-resolution transmission electron microscopy (HRTEM) as shown in Fig. 2. Fig. 2 shows a typical HRTEM image of a microstructure of MWCNTs, indicating that MWCNTs have clear graphite layers. The average pore width and the average thickness of the CNT1 are estimated to be 7.3 and 18.8 nm, respectively. The average pore and the average thickness of the CNT2 are 11.2 and 28 nm, respectively. There are no fine spherical particles, such as soots or catalysts in these two multiwall carbon nanotubes. However, there is an exterior layer on CNT2 observed by electron microscopy that is not present

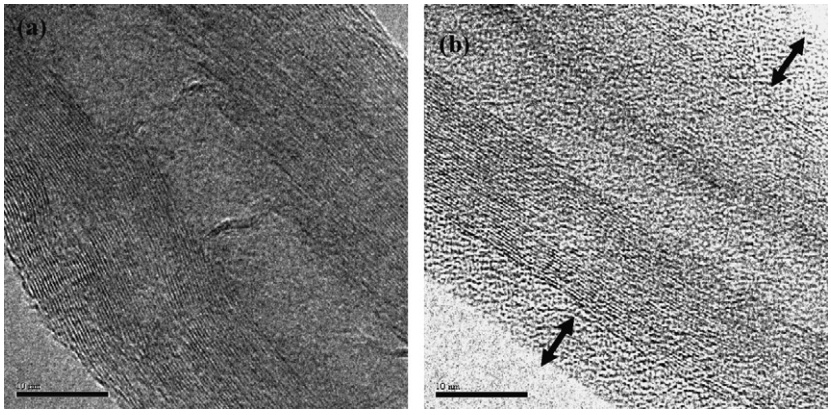

Fig. 2. HRTEM images of (a) CNT1 and (b) CNT2. Arrows show the exterior layers on CNT2.

Table 2
Physical properties of CNT1 and CNT2

	CNT1	CNT2
BET surface area (m^2/g)	108	114
BET average pore size (nm)	10.9	10.2
Mesopore volume (cm^3/g)	0.529	0.430
Micropore volume (cm^3/g)	0.00614	0.00222

on CNT1. According to the EDX spectrum, this coating layer is composed only by carbon atoms. Yang and Xing [23] also indicated that MWCNTs may contain impurities dominated by amorphous carbon.

3.2. Nitrogen adsorption isotherm

Fig. 3 shows the sorption isotherms of nitrogen on these two MWCNTs at 77 K and relative pressures ($P/P_o = 4.04 \times 10^{-5}$ to 0.995). At low P/P_o, the isotherms are of type II, which also includes features of a type I due to micropores. They follow a substantial increase in the uptake of nitrogen due to capillary condensation. The slight hysteresis may result from the intertubular space. The adsorption/desorption isotherms indicated that adsorption of nitrogen on these two CNTs is a reversible reaction. The same type of isotherms have also been reported on multiwalled CNTs [24–26].

Nitrogen adsorption is frequently used to probe porosity and surface area of porous materials. The specific surface area of MWCNTs was calculated by the standard BET method. Table 2 shows the specific surface area and pore volume of CNT1 and CNT2. The mesopore (2–50 nm) volume is dominant in these two nanotubes. The micropore (<2 nm) volume for CNT1 is only

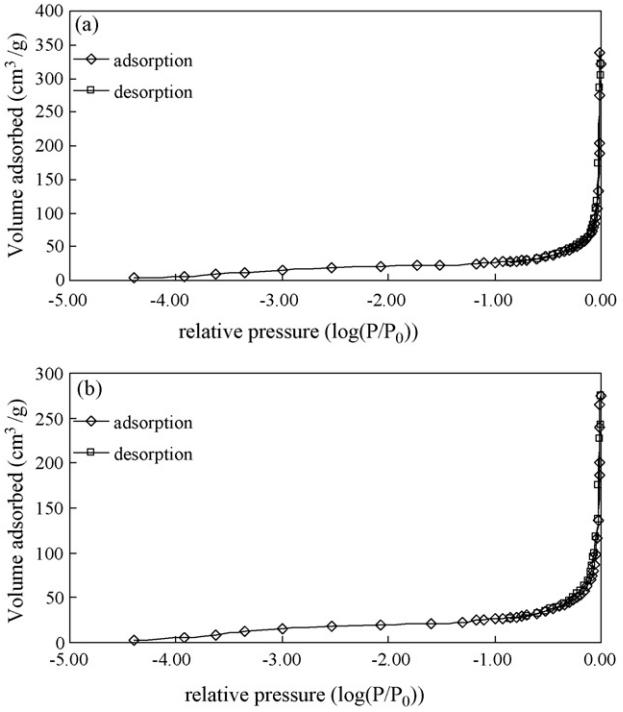

Fig. 3. Nitrogen adsorption isotherms of (a) CNT1 and (b) CNT2 at 77 K.

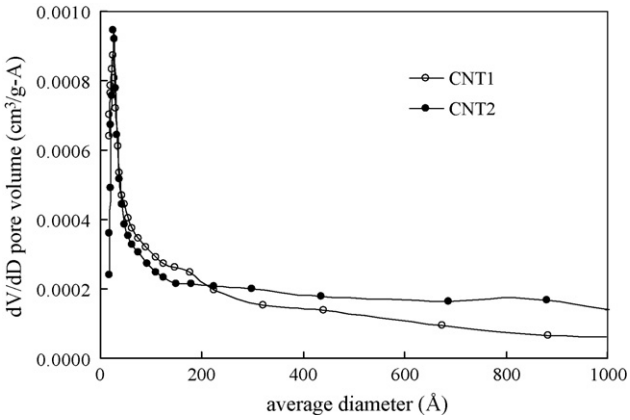

Fig. 4. The pore size distribution of two MWCNTs.

slight more than CNT2. In the pore size distribution plot (Fig. 4), inner hollow cavities mainly 3.0–4.0 nm were observed in these two multiwalled carbon nanotubes. Yang et al. [27] also observed inner hollow cavities of smaller diameter (narrowly distributed, mainly 3.0–4.0 nm) in their MWCNTs. There is no significant difference observed in surface physical properties between these two MWCNTs except for the exterior amorphous carbon layer on CNT2.

3.3. Spectral analysis

Raman spectroscopy is mainly used to characterize crystallinities of carbon nanotubes. All carbon forms contribute to the Raman spectra in the range of 1000–1700 cm^{-1} giving rise to a three-band feature with peaks at ~1350 cm^{-1} (D band), ~1582 cm^{-1} (G band), and ~1615 cm^{-1} (D' band) [28]. The D band is a double-resonance band, which serves as a measure of structural disorder due to finite particle size [29], curvature effects of the graphene, defects caused by pentagons or heptagons, and graphitic or nanoscale carbon particulate material on the tubes [30,31]. The D' band is also a double-resonance Raman feature induced by disorder and defects. The G band results from intramolecular vibration between carbon atoms and the in-plane stretching of the C–C bonds in graphene [29,32]. Behler et al. [28] also indicated that the D band position and the ratio of I_D/I_G depends on the excitation energy of the incident laser energies because of the different resonant Raman effect induced by different excitation energies.

In Fig. 5, the relative intensity of the peaks at 1380 cm^{-1} (D band) and 1550 cm^{-1} (G band) with the laser of wavelength 632.8 nm gives information on the presence of diamond and graphite forms of carbon, respectively [28,33,34]. In addition, the D' band was found at around 1615 cm^{-1}, indicating the defects along the tube body [35]. This D band is induced by disorder or crystallographic defects located in the nanotube walls and ends [36,37]. The ordering of tube walls increases as the ratio of the D band to G band intensity (I_D/I_G ratio) decreases [28]. The I_D/I_G ratio of CNT2, 1.43, is larger than that of CNT1, 1.12, indicating that there is less ordering of the graphite tube walls of CNT2 than CNT1. This is consistent with the above HRTEM observation. For MWCNTs, the I_D/I_G ratio of around

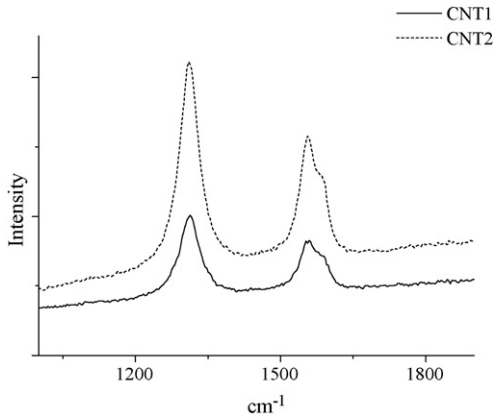

Fig. 5. Raman spectra of two MWCNTs.

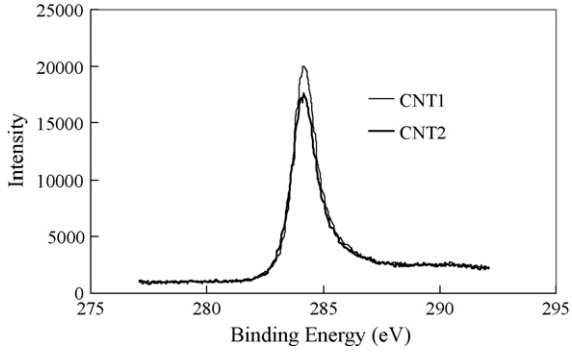

Fig. 6. C1s XPS spectra of two MWCNTs.

1.3–1.6 was also found in some literature [38,39]. In Raman spectra, the peak (D band) is not weak, and the ratio of I_D/I_G is larger than 1, revealing large amount of disordered carbon in these two MWCNTs.

XPS was also performed on these two carbon nanotubes for surface chemical analysis (Fig. 6). The carbon 1s peak in XPS spectra can be resolved into three assignments [40]: 284.38–284.53 eV for C=C bindings, 285.11–285.5 eV, C–C bindings, and 286.21–287.53 eV for C–O bindings. The distribution of C in each structural group was calculated as the percentage to the total carbon. The C–O bindings are 11.8 and 13.1% for CNT1 and CNT2, respectively.

3.4. Adsorption of VOCs on MWCNTs

The adsorption coefficients of four VOCs on MWCNTs at 303 K are shown in Table 3. The adsorption coefficients of acetone, the most polar compound in this study, are the largest for these two carbon nanotubes. Acetone molecules may occur at specific interactions on these two MWCNTs due to their curvature and topological defects. The high I_D/I_G ratio of these two multiwall carbon nanotubes as compared to single carbon nanotubes indicates more structurally disordered walls and defects on these two MWCNTs. Several studies have indicated that defect sites are of great importance to the adsorption process [20,41–43]. On curvature and topological defects, acetone may lead to a chemical adsorption on carbon nanotubes [20]. Chakrapani et al. [20] presented the strong chemisorption of acetone molecules on the surface of carbon nanotubes with a Stone-Wales defect. Tang et al. [44] indicated that carbon nanotubes can adsorb one polar compound, water molecule, by electrostatic interaction. They suggested that carbon nanotubes act as an electric dipole with water molecules serving as electron donors. Acetone dipoles have also been suggested to produce dipole-dipole interactions on planar graphite [45].

For the adsorption of three hydrophobic compounds, trichloroethylene, *n*-hexane, and benzene on CNT1, the adsorption coefficients are around 4 and 5 (L/g) for three hydrophobic compounds, trichloroethylene, *n*-hexane, and benzene. The adsorption coefficients of organic compounds on carbon nanotubes around 2–10 (L/g) have been reported [10,46]. The adsorption coefficients of these three adsorbates seem to decrease slightly with a decreasing trend of their molecular weight, suggesting that van der Waals interactions dominate the sorption process between these three adsorbates and surface of CNT1. It has been suggested that the dispersive interactions of several VOCs on MWCNTs mainly control the adsorption process [24]. However, the adsorption coefficients we report decrease in the order benzene ≒ trichloroethylene > *n*-hexane on CNT2. The molecular descriptors of dipolarity, electron donor and electron acceptor of benzene and trichloroethylene shown in Table 1 are larger than those of *n*-hexane. This indicates that the surface of CNT2 is favorable for the π–π electron donor–acceptor (EDA) interaction with adsorbates. The EDA interactions between organic adsorbates and carbon nanotubes have been presented by several studies [5,47,48]. Díaz et al. [24] also indicated that specific interactions of benzene larger than cyclohexane on multiwalled CNTs may be caused by the π carbon–carbon interaction.

The adsorption capacities of CNT1 for all organic vapors were less than the corresponding values for CNT2. Adsorption of organic vapors on carbon nanotubes can occur in the hollow space inside nanotubes, the interstitial space between nanotubes, and the curved surface of nanotube bundles [46]. Organic chem-

Table 3
Adsorption coefficients of the four selected VOCs on MWCNTs at various temperatures

K (L/g)	303 K		333 K		363 K	
	CNT1	CNT2	CNT1	CNT2	CNT1	CNT2
Trichloroethylene	5.24 ± 0.358	24.9 ± 0.887	1.50 ± 0.251	14.1 ± 6.81	0.778 ± 0.270	5.76 ± 1.19
Benzene	3.56 ± 0.335	25.5 ± 0.915	1.25 ± 0.260	8.3 ± 2.87	0.802 ± 0.270	2.26 ± 0.233
n-Hexane	4.21 ± 0. 314	16.7 ± 1.31	1.41 ± 0.286	11.4 ± 6.95	0.888 ± 0.286	2.72 ± 1.07
Acetone	75.9 ± 0.170	516.4 ± 1.42	10.7 ± 1.55	43.9 ± 0.370	2.84 ± 0.266	5.83 ± 0.497

Table 4
Adsorption enthalpies (ΔH) of the four selected VOCs on MWCNTs

	TCE	*n*-Hexane	Benzene	Acetone
ΔH_{CNT1} (kJ/mol)	−29.3	−23.9	−22.9	−49.9
ΔH_{CNT2} (kJ/mol)	−20.3	−35.3	−38.1	−68.3

icals in this study do not enter into the MWCNT layers because these organic chemicals are too large to be adsorbed in the spaces between layers of MWCNTs. Agnihotri et al. [46] suggested that the organic vapor adsorption would mainly occur inside the nanotubes and then on the external surface of CNT bundles. According to our pore size distribution, organic vapor adsorption can occur inside the nanotubes and the external surface of these two MWCNT bundles. The slightly greater surface area of CNT2 than CNT1 (Table 2) may be responsible for a minor part of the higher adsorption capacity of CNT2. The main cause could be the amorphous carbon layer on the surface of CNT2 (Fig. 2). Hilding and Grulke [41] also indicated that amorphous carbon associated with raw carbon nanotubes is a strong adsorbent for hydrocarbons.

3.5. Thermodynamics of VOCs on MWCNTs

The adsorption capacity of these VOCs decreased with increased temperature, as shown in Table 3. Whether the adsorption of VOCs on MWCNTs is due to a physical or a chemical process can be elucidated via the measured enthalpy change (ΔH). Applying the van't Hoff equation, the relationship between the change of enthalpy and adsorption coefficients can be quantified as

$$\frac{\mathrm{d}\ln K}{\mathrm{d}T} = \frac{\Delta H}{RT^2} \quad (5)$$

where R is the ideal gas constant, T is the absolute temperature (K), and K is the equilibrium MWCNTs-gas distribution coefficient.

Assuming that ΔH is constant over the studied temperature range, relatively low negative values of enthalpy change are obtained (Fig. 7), ranging from −20 to −38 kJ/mol for the three nonpolar hydrophobic chemicals, trichloroethylene, benzene, and *n*-hexane (Table 4). This implies that the adsorption processes of these three hydrophobic chemicals are physical, exothermic processes. The adsorption enthalpies of these three adsorbates on MWCNT previously measured [24] are similar to our results. This is in agreement with physical adsorption of nonpolar organic vapors on carbon nanotubes [24,41,46].

The adsorption enthalpies for CNT2 were generally greater than those for CNT1 indicating that the interaction of these organic vapors with CNT2 was stronger than CNT1. This may be due to the presence of the exterior carbonaceous layers on CNT2.

The heats of adsorption of benzene and *n*-hexane on MWCNTs in this study are lower than those on SWCNT and on graphite [8,46,49,50]. The heat of adsorption for a gas adsorbed on SWCNTs is generally higher than on planar graphite and on MWCNTs [41]. The highly bent graphite sheet on the SWCNT

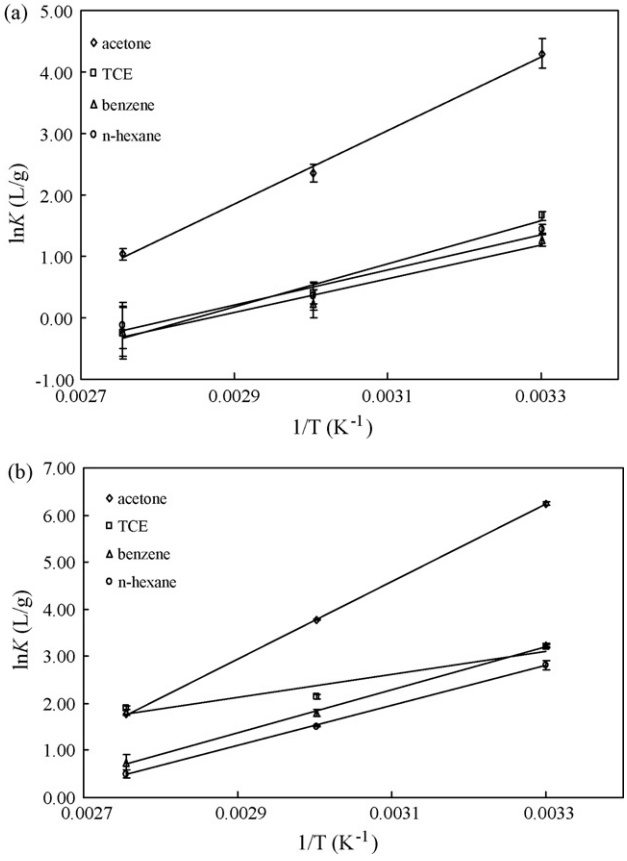

Fig. 7. Adsorption enthalpies of these selected VOCs on (a) CNT1 and (b) CNT2. For CNT1, $\ln K_{acetone} = 6000(1/T) - 15.6$ with $R^2 = 0.997$, $\ln K_{TCE} = 3520(1/T) - 10.0$ with $R^2 = 0.984$, $\ln K_{n\text{-hexane}} = 2878(1/T) - 8.14$ with $R^2 = 0.970$ and $\ln K_{benzene} = 2757(1/T) - 7.90$ with $R^2 = 0.968$. For CNT2, $\ln K_{acetone} = 8220(1/T) - 20.9$ with $R^2 = 0.999$, $\ln K_{TCE} = 2443(1/T) - 4.95$ with $R^2 = 0.915$, $\ln K_{n\text{-hexane}} = 4246(1/T) - 11.2$ with $R^2 = 0.999$ and $\ln K_{benzene} = 4569(1/T) - 11.9$ with $R^2 = 0.999$.

wall has strained double bonds. This gives SWCNTs a higher surface potential inside the pores and on the outer wall than on a flat graphite surface [51]. These enthalpy results indicate that the surface strain on MWCNTs is not sufficient to create the sp^2/sp^3 orbit-hybridization that can be observed in SWCNTs.

The observation of the largest adsorption enthalpy of acetone indicates that some chemical bond may be formed or broken during sorption and desorption, which is in agreement with the literature [20]. This value is larger than the enthalpy of adsorption of acetone on graphitized carbon (31.3 kJ/mol) [52]. In our TPD experiments, there were no identifiable peaks for *n*-hexane, benzene or trichloroethylene after purging with helium gas on either MWCNT therefore no desorption energies could be calculated. This suggests that there were no strong interactions between these chemicals and the MWCNTs. However, desorption peaks were observed for acetone with both of the MWCNTs used in this study. The desorption activation energies calculated for acetone in our system were 169.2 and 94.9 kJ/mol for CNT1 and CNT2, respectively (Fig. 8). This indicates that strong interactions occurred between acetone molecules and the carbon nanotubes. Using temperature-programmed desorption experiments and theoretical computer simulations, Chakrapani

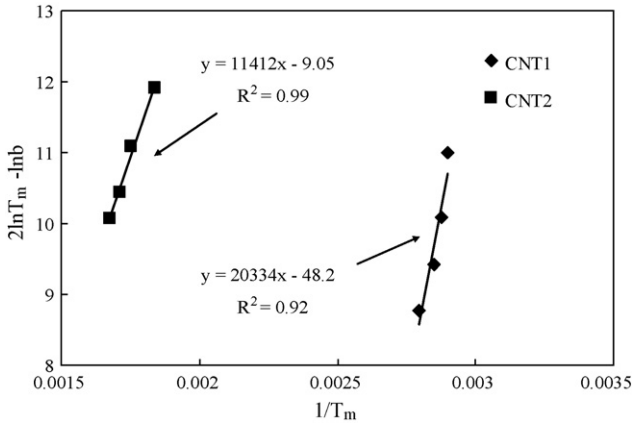

Fig. 8. Relationship between the maximum desorption temperature and the heating rate for acetone on two MWCNTs.

et al. [20] have reported that chemisorption of acetone occurs on carbon nanotube surface due to the effects of curvature and topological defects of the nanotubes. They also found the presence of oxygen in their pristine carbon nanotube. The defects are likely to be reactive to acetone molecules since chemisorption generally causes a higher adsorption enthalpy change. The existence of some defects in the carbon nanotubes shown in our XPS results is the most likely factor for explaining the apparent chemisorption we observed.

4. Conclusion

Four VOCs, acetone, trichloroethylene, benzene, and *n*-hexane, were used as chemical probes to investigate the adsorption mechanisms of MWCNTs, CNT1 and CNT2, at room temperature (303 K). Amorphous carbon on the exterior layers of CNT2 was observed by electron microscopy. The adsorption coefficients of VOCs on CNT2 were larger than those on CNT1, suggesting that the amorphous carbon on MWCNTs provided more sorption capacity for organic chemicals. The sorption equilibrium coefficients of acetone on both MWCNTs were found to be higher than other VOC compounds. This may result from the strong chemical interactions of acetone molecules to the topological defects and disorder in MWCNTs observed by Raman spectra. The adsorption equilibrium coefficients of these VOC compounds decreased with increasing temperature between 303 and 363 K, indicating that the sorption process is exothermic for these four VOCs on both MWCNTs. Trichloroethylene, benzene, and *n*-hexane all performed physisorption on the MWCNT surface. The high sorption heats and desorption activation energies of acetone show that acetone might chemisorb on both MWCNTs. The curvature and topological defects affect the sorption mechanism of organic compounds on carbon nanotubes.

Acknowledgements

We gratefully acknowledge the financial support of the National Science Council of Taiwan, Republic of China (Contracts NSC 93-2313-B-005-088 and NSC 94-2313-B-005-064). This work is supported in part by the Ministry of Eduction, Taiwan, R.O.C., under the ATU plan.

References

[1] S. Iijima, Helical microtubules of graphitic carbon, Nature 354 (1991) 56.
[2] C. Kim, Y.S. Chio, S.M. Lee, J.T. Park, B. Kim, Y.H. Lee, The effect of gas adsorption on the field emission mechanism of carbon nanotubes, J. Am. Chem. Soc. 124 (2002) 9906.
[3] R.O. Dillon, J.A. Woollam, V. Katanant, Use of Raman scattering to investigate disorder and crystallite formation in as-deposited and annealed carbon films, Phys. Rev. B 29 (1984) 3482.
[4] M.D. Ellison, M.J. Crotty, D. Koh, R.L. Spray, K.E. Tate, Adsorption of NH_3 and NO_2 on single-walled carbon nanotubes, J. Phys. Chem. B 08 (2004) 7938.
[5] J. Zhang, J.K. Lee, V. Wu, R.W. Murray, Photoluminescence and electronic interaction of anthracene derivatives adsorbed on sidewalls of single-walled carbon nanotubes, Nano. Lett. 3 (2003) 403.
[6] P. Kondratyuk, J.T. Yates Jr., Desorption kinetic detection of different adsorption sites on opened carbon single walled nanotubes: the adsorption of *n*-nonane and CCl_4, Chem. Phys. Lett. 410 (2005) 324.
[7] R.Q. Long, R.T. Yang, Carbon nanotubes as superior sorbent for dioxin removal, J. Am. Chem. Soc. 123 (2001) 2058.
[8] D. Crespo, R.T. Yang, Adsorption of organic vapors on single-walled carbon nanotubes, Ind. Eng. Chem. Res. 45 (2006) 5524.
[9] X. Peng, Y. Li, Z. Luan, Z. Di, H. Wang, B. Tian, Adsorption of 1,2-dichlorobenzene from water to carbon nanotubes, Chem. Phys. Lett. 376 (2003) 154.
[10] K. Yang, L. Zhu, B. Xing, Adsorption of polycyclic aromatic hydrocarbon by carbon nanomaterials, Environ. Sci. Technol. 40 (2006) 1885.
[11] K.U. Goss, R.P. Schwarzenbach, Adsorption of a diverse set of organic vapors on quartz, $CaCO_3$ and α-Al_2O_3 at different relative humidities, J. Colloid Interface Sci. 252 (2002) (2002) 31.
[12] C.M. Roth, K.-U. Goss, R.P. Schwarzenbach, Sorption of a diverse set of organic vapors to diesel soot and road tunnel aerosols, Environ. Sci. Technol. 39 (2005) 6632.
[13] R.T. Yang, Gas Separation by Adsorption Processes, Butterworths, Boston, 1997.
[14] J.R. Conder, C.L. Young, Physicochemical Measurements by Gas Chromatography, Wiley, New York, 1979.
[15] E. Papirer, E. Brendle, F. Ozil, H. Balard, Comparison of the surface properties of graphite, carbon black and fullerence samples, measured by inverse gas chromatography, Carbon 37 (1999) 1265.
[16] F. Thielmann, D.A. Butler, D.R. Williams, Characterization of porous materials by finite concentration inverse gas chromatography, Colloid Surf. A Physicochem. Eng. Asp. 187–188 (2001) 267.
[17] S. Tain, L. Zhu, Y. Shi, Characterization of sorption mechanisms of VOCs with organobentonites using a LSER approach, Environ. Sci. Technol. 38 (2004) 489.
[18] M. Kazayawoko, J. Balatinecz, M. Romansky, Thermodynamics of adsorption of *n*-alkanes on maleated wood fibers by inverse gas chromatography, J. Colloid Interface Sci. 190 (1997) 408.
[19] R.T. Yang, R.Q. Long, J. Padin, A. Takahashi, T. Takahashi, Adsorbents for dioxins: a new technique for sorbent screening for low-volatile organics, Ind. Eng. Chem. Res. 38 (1999) 2726.
[20] N. Chakrapani, Y.M. Zhang, S.K. Nayak, J.A. Moore, D.L. Carroll, Y.Y. Choi, P.M. Ajayan, Chemisorption of acetone on carbon nanotubes, J. Phys. Chem. B 107 (2003) 9308.
[21] J. Park, R.T. Yang, Predicting adsorption isotherms of low-volatile compounds by temperature programmed desorption: iodine on carbon, Langmuir 21 (2005) 5055.
[22] R.J. Cvetanovic, Y. Amenomiya, Application of a temperature-programmed desorption technique to catalyst studies, Adv. Catal. 17 (1967) 103.
[23] K. Yang, B. Xing, Desorption of polycyclic aromatic hydrocarbons from carbon nanomaterials in water, Environ. Pollut. 145 (2007) 529.

[24] E. Díaz, S. Ordóñez, A. Vega, Adsorption of volatile organic compounds onto carbon nanotubes, carbon nanofibers, and high-surface-area graphites, J. Colloid Interface Sci. 305 (2007) 7.
[25] C. Gommes, S. Blacher, N. Dupont-Pavlovsky, C. Bossuot, M. Lamy, A. Brasseur, Comparison of different methods for characterizing multi-walled carbon nanotubes, Colloid Surf. A Physicochem. Eng. Asp. 241 (2004) 155.
[26] Z. Li, Z. Pan, S. Dai, Nitrogen adsorption characterization of aligned multiwalled carbon nanotubes and their acid modification, J. Colloid Interface Sci. 277 (2004) 35.
[27] Q.H. Yang, P.X. Hou, S. Bai, M.Z. Wang, H.M. Cheng, Adsorption and capillarity of nitrogen in aggregated multi-walled carbon nanotubes, Chem. Phys. Lett. 345 (2001) 18.
[28] K. Behler, S. Osswald, H. Ye, S. Dimovski, Y. Gogotsi, Effect of thermal treatment on the structure of multi-walled carbon nanotubes, J. Nanoparticle Res. 8 (2006) 615.
[29] H. Hiura, T.W. Ebbesen, K. Tanigaki, Raman studies of carbon nanotubes, Chem. Phys. Lett. 202 (1993) 509.
[30] W.S. Bacas, D. Ugarte, A. Chatelain, W.A. de Heer, High-resolution electron microscopy and inelastic light scattering of purified multishelled carbon nanotubes, Phys. Rev. B 50 (1994) 473.
[31] P.C. Eklund, J.M. Holden, R.A. Jishi, Vibrational modes of carbon nanotubes: spectroscopy and theory, Carbon 33 (1995) 959.
[32] Y.F. Wang, X.W. Cao, S.F. Hu, Y.Y. Liu, G.X. Lan, Graphical method for assigning Raman peaks of radial breathing modes of single-walled carbon nanotubes, Chem. Phys. Lett. 336 (2001) 47.
[33] M.S. Dresselhaus, M.A. Pimenta, P.C. Eklund, Raman scattering in fullerenes and related carbon-based materials, in: W.H. Weber, R. Merlin (Eds.), Raman Scattering in Materials Sciences, Springer-Verlag, New York, 2000, pp. 314–364.
[34] A.C. Dillon, K.M. Jones, T.A. Bekkedahl, C.H. Kiang, D.S. Bethune, M.J. Heben, Storage of hydrogen in single-walled carbon nanotubes, Nature 386 (1997) 377.
[35] A. Jorio, M.A. Pimenta, A.G. Souza Filho, R. Saito, G. Dresselhaus, M.S. Dresselhaus, Characterizing carbon nanotube sample with resonance Raman scattering, New J. Phys. 5 (2003) 1.
[36] W.S. Bacsa, D. Ugarte, A. Châtelain, W.A. de Heer, High-resolution electron microscopy and inelastic light scattering of purified multishelled carbon nanotubes, Phys. Rev. B 50 (1994) 15473.
[37] A. Kasuya, Y. Sasaki, Y. Saito, K. Tohji, Y. Nihjina, Evidence for size-dependent discrete dispersions in single-wall nanotubes, Phys. Rev. Lett. 78 (1997) 4434.
[38] M.J. Park, J.K. Lee, B.S. Lee, LeeF Y.-W., I.S. Choi, S.-g. Lee, Covalent modification of multiwalled carbon nanotubes with imidazolium-based ionic liquids: effect of anions on solubility, Chem. Mater. 18 (2006) 1546.
[39] A.M. Shanmugharaja, J.H. Bae, K.Y. Lee, W.H. Noh, S.H. Lee, S.H. Ryu, Physical and chemical characteristics of multiwalled carbon nanotubes functionalized with aminosilane and its influence on the properties of natural rubber composites, Compos. Sci. Technol. 67 (2007) 1813.
[40] T.I.T. Okapalugo, P. Papakonstaninuo, H. Murphy, J. McLaughlin, N.M.D. Brown, High resolution XPS characterization of chemical functionalized MWCNTs and SWCNTs, Carbon 43 (2005) 153.
[41] J.M. Hilding, E.A. Grulke, Heat of adsorption of butane on multiwalled carbon nanotubes, J. Phys. Chem. B 108 (2004) 13688.
[42] L.G. Zhou, S.Q. Shi, Adsorption of foreign atoms on Stone-Wales defects in carbon nanotube, Carbon 41 (2003) 579.
[43] H.B. Zhang, G.D. Lin, S.H. Zhou, X. Dong, T. Chen, Raman spectra of MWCNT and MWCNT-based H_2-adsorbing, Carbon 40 (2002) 2429.
[44] D. Tang, L. Ci, W. Zhou, S. Xie, Effect of H_2O adsorption on the electrical transport properties of double-walled carbon nanotubes, Carbon 44 (2006) 2155.
[45] S. Kwon, J. Russell, X. Zhao, R.D. Vidic, Combined experimental and theoretical investigation of polar organic adsorption/desorption from model carbonaceous surfaces: acetone on graphite, Langmuir 18 (2002) 2595.
[46] S. Agnihotri, M.J. Rood, M. Rostam-Abadi, Adsorption equilibrium of organic vapors on single-walled carbon nanotubes, Carbon 43 (2005) 2379.
[47] R.J. Chen, Y. Zhang, D. Wang, H. Dai, Noncovalent sidewall functionalization of single-walled carbon nanotubes for protein immobilization, J. Am. Chem. Soc. 123 (2001) 3838.
[48] H. Li, B. Zhou, Y. Lin, L. Gu, W. Wang, S. Fernando, S. Kumar, L.F. Allard, Y.P. Sun, Selective interactions of porphyrins with semiconducting single-walled carbon nanotubes, J. Am. Chem. Soc. 126 (2004) 1014.
[49] M. Eswaramoorthy, R. Sen, C.N.R. Rao, A study of micropores in single-walled carbon nanotubes by the adsorption of gases and vapors, Chem. Phys. Lett. 340 (1999) 207.
[50] J.W. Grate, M.H. Abraham, C.M. Du, R.A. McGill, W.J. Shuely, Examination of vapor sorption by fullerene, fullerene-coated surface acoustic wave sensors, graphite, and low-polarity polymers using linear solvation energy relationships, Langmuir 11 (1995) 2125.
[51] S.M. Gatica, M. Boninsegni, S. Curtarolo, M.W. Cole, Atoms in nanotubes: small dimensions and variable dimensionality, Am. J. Phys. 67 (1999) 1170.
[52] P.A. Elkington, G. Curthoys, Heats of adsorption on carbon black surfaces, J. Phys. Chem. 73 (1969) 2321.
[53] M.H. Abraham, P.L. Grellier, R.A. McGill, Determination olive oil-gas and hexadecane–gas partition coefficients, and calculation of the corresponding olive oil–water and hexadecane–water partition coefficients, J. Chem. Soc. Perkin Trans. 2 (1987) 797.